Monografías Matemáticas *García de Galdeano* **41**, 85–94 (2018)

NUMERICAL APPROXIMATION OF SINGULARLY PERTURBED REACTION-DIFFUSION PROBLEMS WITH THE VIRTUAL ELEMENT METHOD

José Luis Gracia and Diego Irisarri

Abstract. In this paper we approximate 2D reaction-diffusion elliptic singularly perturbed problems with the virtual element method. This method is combined with the link-cutting technique in order to obtain a stable solution but it is only accurate outside the layer regions. We use a post-processing technique to approximate the solution in the layer regions. Numerical results show the robustness of the method with respect to the diffusion parameter if a suitable graded mesh is used in the layer regions.

Keywords: Virtual element method, reaction-diffusion problem, singularly perturbed problem, boundary and corner layers, post-processing technique.

AMS classification: 65L11, 65N30.

§1. Introduction

Singular perturbation problems arise in many practical applications. The solution of these problems exhibits a multi-scale character and, therefore, classical numerical methods fail to obtain accurate approximations to the solution, unless a very fine (which depends adversely on the singular perturbation parameter) mesh is considered. Finite difference and finite element methods have been used in the literature to approximate singularly perturbed problems (see [14] and the references therein) but up to our knowledge, except in [12], the virtual element method (VEM) has not been used yet in the literature for its numerical approximation.

In this paper we use VEM to approximate the solution of singularly perturbed problems of reaction-diffusion type. This method arises from the mimetic difference methods but it is formulated in the framework of the finite element method (FEM). In fact, it can be considered as a generalization of the FEM. For a general overview we refer to [2, 5] and this method has been applied both to linear elasticity problems [4, 8] and fluid mechanics [3, 6], for instance.

In [12], using the flexibility of the VEM meshes, a methodology was developed to obtain a stable solution modifying the mesh via the link-cutting condition. This method damps out the spurious oscillations and provides an accurate solution in the whole domain except inside the layers regions if one uses a coarse triangulation compared to the singular perturbation parameter ε. In this paper we propose to use a post-processing technique to improve the solution in the layer regions and it can be viewed as a variant of the Schwartz iterative technique. With this aim, we solve the problem in a subdomain of thickness $O(\sqrt{\varepsilon})$ which overlaps the layer regions and whose boundary conditions are appropriately defined. We refer to this problem in this paper as the local problem. In spite of solving in the layer regions,

the numerical results suggest that the method is uniformly convergent in the maximum norm if a graded mesh is used to approximate the local problem. Extensive numerical results on polygonal domains have been performed in [13] but here, for the sake of clarity, we describe our method for reaction-diffusion problems in a rectangular domain.

§2. Virtual element method discretization

Consider the following two-dimensional Dirichlet boundary value reaction-diffusion problem

$$\begin{cases} -\varepsilon\Delta u + b(x,y)u &= f(x,y), \qquad \text{for} \quad (x,y)\in\Omega, \\ u &= 0 \qquad\qquad\quad \text{on} \quad \Gamma, \end{cases} \tag{1}$$

where Ω is a polygonal domain in $\mathbb{R}^2$ with boundary Γ. We assume that the reaction term satisfies $b(x,y)\geq\beta>0$ for $(x,y)\in\bar{\Omega}$, b and f are sufficiently smooth functions and $0<\varepsilon\leq 1$. The coefficient ε is called the singular perturbation parameter.

The variational formulation of problem (1) reads: Find $u\in V=H_0^1(\Omega)$ such that

$$B(u,v)=(f,v), \quad \forall v\in V, \tag{2}$$

where

$$B(u,v)=a(u,v)+c(u,v), \tag{3}$$

and

$$a(u,v)=\int_\Omega \varepsilon\,\nabla u\cdot\nabla v, \quad c(u,v)=\int_\Omega b\,u\,v, \quad (f,v)=\int_\Omega f\,v. \tag{4}$$

A detailed discussion on the discretization of the variational problem (2) with the VEM can be found in [3]. We only give a brief description of the basic features of this method below.

The domain Ω is first decomposed into a partition $\mathcal{P}_h$ composed of polygons K, and let $\mathcal{E}_h$ be the set of edges e of $\mathcal{P}_h$. We consider on each element K the following space for linear elements

$$\widetilde{V}_h(K)=\left\{v\in H^1(K):\ v_{|e}\in\mathbb{P}_1(e)\ \forall\, e\subset\partial K, \Delta v\in\mathbb{P}_1(K)\right\}.$$

This is the space of the functions that are linear on each edge and hence they are completely determined by their values at the vertices of K. Inside $\widetilde{V}_h(K)$, the functions are harmonic and its total dimension is equal to the number of vertices of K. For higher order elements, the degrees of freedom are different [3].

A crucial ingredient in the construction of a suitable local stiffness matrix (ensuring consistency and stability) is the projection operator $\Pi_1^\nabla:\widetilde{V}_h(K)\to\mathbb{P}_1(K)$, defined, for every $v\in\widetilde{V}_h(K)$, as the solution of

$$\int_K\nabla(\Pi_1^\nabla v-v)\cdot\nabla p=0,\ \forall p\in\mathbb{P}_1(K) \ \text{ and } \ \int_{\partial K}(\Pi_1^\nabla v-v)=0, \tag{5}$$

and therefore the polynomial $\Pi_1^\nabla v$ can be computed using the degrees of freedom (i.e., the values of v at the vertices of K).

We now introduce the local virtual element space for linear elements

$$V_h(K) = \left\{ v \in \widetilde{V}_h(K) : \int_K v\, p = \int_K \Pi_1^\nabla v\, p, \quad \forall p \in \mathbb{P}_1(K) \right\}. \tag{6}$$

The global finite dimensional virtual element space is then defined as

$$V_h = \{ v \in V : v_{|K} \in V_h(K)\ \forall K \in \mathcal{P}_h \}. \tag{7}$$

We denote by Π_k^0 the L^2-projection from V_h onto $\mathbb{P}_k$, defined locally as

$$\int_K (v - \Pi_k^0 v)\, p_k = 0 \quad \forall p_k \in \mathbb{P}_k(K). \tag{8}$$

The bilinear form expressed in (4) can be discretized as the sum of the bilinear forms restricted to the elements. Therefore, for all $u, v \in V_h$

$$B_h(u, v) = a_h(u, v) + c_h(u, v), \tag{9}$$

with

$$a_h(u, v) = \sum_{K \in \mathcal{P}_h} a_h^K(u, v),\ c_h(u, v) = \sum_{K \in \mathcal{P}_h} c_h^K(u, v), \tag{10}$$

the elemental bilinear forms are given by

$$\begin{aligned} a_h^K(u, v) &= \int_K \varepsilon [\Pi_0^0 \nabla u] \cdot [\Pi_0^0 \nabla v] + S_\varepsilon^K((I - \Pi_1^\nabla)u, (I - \Pi_1^\nabla)v), \\ c_h^K(u, v) &= \int_K b [\Pi_1^0 u][\Pi_1^0 v] + S_b^K((I - \Pi_1^0)u, (I - \Pi_1^0)v), \end{aligned} \tag{11}$$

and the terms $S_\varepsilon^K(\cdot, \cdot)$ and $S_b^K(\cdot, \cdot)$ are defined in (14). The right-hand side of (2) is approximated by

$$(f_h, v_h) = \sum_{K \in \mathcal{P}_h} (f_h, v_h)_K = \sum_{K \in \mathcal{P}_h} \int_K \Pi_1^0 f v_h. \tag{12}$$

As we have considered linear elements, the degrees of freedom, $\mathrm{dof}_i(\cdot)$, are the values of v_h at the vertex i for $i = 1, \ldots, n$ where n is the number of vertices of $\mathcal{P}_h$. The basis functions $\varphi_i \in V_h$ are defined as the canonical basis functions, and they satisfy

$$\mathrm{dof}_i(\varphi_j) = \delta_{ij}, \quad i, j = 1, ..., n. \tag{13}$$

Thus,

$$v_h = \sum_{i=1}^{n} \mathrm{dof}_i(v_h)\varphi_i \quad v_h \in V_h\,.$$

The terms $S_\varepsilon^K(\cdot, \cdot)$ and $S_b^K(\cdot, \cdot)$ in (11) guarantee the stability of the method. They are given by [5]

$$S_\varepsilon^K((I - \Pi_k^\nabla)\varphi_i, (I - \Pi_k^\nabla)\varphi_j) = \varepsilon[(I - \Pi_k^\nabla)^T (I - \Pi_k^\nabla)]_{ij}\,, \tag{14a}$$

$$S_b^K((I - \Pi_k^\nabla)\varphi_i, (I - \Pi_k^\nabla)\varphi_j) = b|K|[(I - \Pi_1^0)^T (I - \Pi_1^0)]_{ij}\,. \tag{14b}$$

Then, the discrete problem can be written as

$$\begin{cases} \text{Find } \ u_h \in V_h \ \text{ such that} \\ B_h(u_h, v_h) = (f_h, v_h) \ \ \forall v_h \in V_h \end{cases} \tag{15}$$

§3. Numerical methodology

The numerical approximation that we propose in this paper is obtained in two steps. Firstly, a stable solution is obtained by using the VEM described in Section 2 together with the concept of the link-cutting condition. It consists in modifying the mesh such as a stabilized numerical solution is obtained; nevertheless it is an accurate approximation to the problem (1) in the whole domain except in the layer regions. In the second step, we solve a local problem in the layer regions where the values of the boundary conditions are defined by using the solution computed in the previous step. Finally, both solutions are merged. This technique is usually called global/local or zooming methods.

3.1. Step 1: Numerical solution using VEM and link-cutting condition

Following the link-cutting concept [7, 12], we have obtained stable solutions with the VEM by removing the interaction between the basis functions associated with the vertices on the boundary of the domain and the neighbouring basis functions. We give a brief description of this condition: Let Υ_B denote the set of degrees of freedom belonging to the boundary of the domain. Then, the link-cutting condition can be formulated as:

$$\sum_{m \in \Upsilon_B} B_h(\varphi_n, \varphi_m) = 0 \ \ \forall n \notin \Upsilon_B \,, \tag{16}$$

where recall that φ_n are the basis functions of the space $V_h(K)$.

A way of fulfilling (16) is introducing a row of quadrilaterals on the boundary layer regions with a suitable width, which is called the link-cutting distance [12] and it is denoted by σ_{LC} (see Figure 1). For example, the link-cutting condition for the vertex n depicted in Figure 1 would be

$$B_h(\varphi_n, \varphi_{m1}) + B_h(\varphi_n, \varphi_{m2}) + B_h(\varphi_n, \varphi_{m3}) = 0. \tag{17}$$

In the case of a constant coefficient problem with $b(x, y) \equiv b$, the link-condition distance for the reaction-diffusion problem is given by

$$\sigma_{LC} = \sqrt{\frac{6\varepsilon}{b}},$$

and (16) is satisfied exactly. In the case of a variable coefficient problem, we take the link-cutting distance as the natural extension

$$\sigma_{LC} = \sqrt{\frac{6\varepsilon}{\min_\Gamma(b)}} \,. \tag{18}$$

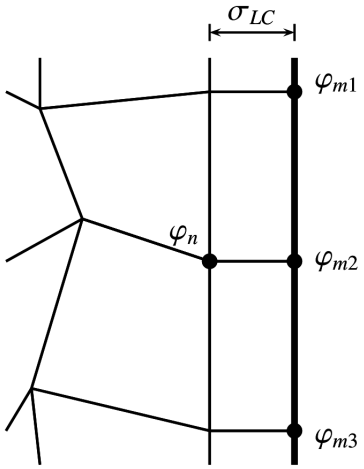

Figure 1: Mesh modification on the boundary layer.

It is worth noting that the value σ_{LC} depends on the data problem but it is irrespective of the length of the quadrilaterals.

The VEM has the advantage with respect to FEM that different type of elements can be used. This peculiarity is very important here because the former computational mesh has been modified with the row of quadrilaterals without taking into account how it affects to the number of vertices of the neighbouring elements.

3.2. Step 2: The post-processing technique and the local problem in the layer regions

The numerical solution computed in the first step provides an accurate approximation to the problem (1) in the outer region but not in the inner region. Thus, the objective of this step is to improve the approximation in the inner region. With this aim, we solve a local problem in the layer regions and the values of the boundary conditions are obtained from the numerical solution computed in the previous step. Once the solutions of the first and second steps are obtained, they are patched to have the final approximation to the solution in the whole domain.

§4. Numerical results

For the sake of clarity, we show our methodology for a test problem defined on the unit square. We have obtained similar results for other polygonal domains [13].

In the case of a rectangular domain, it is well known that the solution exhibits, in general, a boundary layer of order of $O(\sqrt{\varepsilon})$ on each side of the domain and four corner layers in the neighbourhood of the corners of the domain (see [10] for further details in the behaviour of

the solution). We consider a particular example [9] of (1) with the following coefficients

$$-\varepsilon\Delta u + (1+(1-x)^2(1-y)^2)u = 1 + 2(1-x)(1-y), \text{ in } \Omega = (0,1)\times(0,1), \tag{19a}$$

$$u(x,0) = 2x - x^2, \quad u(x,1) = 1, \quad x \in [0,1], \tag{19b}$$

$$u(0,y) = 2y - y^2, \quad u(1,y) = 1, \quad y \in [0,1]. \tag{19c}$$

The boundary conditions have been chosen such that the solution of the problem (19) only has two boundary layers in the vicinity of $x = 0$ and $y = 0$ and a corner layer at the vertex $(0,0)$. We refer to [11] concerning the regularity of the solution u. This test problem satisfies the compatibility conditions of zero level at the four corners of the domain but not the compatibility condition of first level at $(0,0)$ since

$$4\varepsilon = -\varepsilon u_{xx}(0,0) - \varepsilon u_{yy}(0,0) + b(0,0)u(0,0) \neq f(0,0) = 3.$$

Nonetheless, $u \in C^{1,\alpha}(\bar{\Omega})$ (it denotes the Hölder function space of exponent α) and spite of this lack of regularity, we approximate the solution with the scheme given in Section 3.

Step 1: We first define a decomposition $\mathcal{P}_N$ of the domain Ω into square elements. We denote by N the number of elements in each direction. The initial partition of the domain is then modified using the link-cutting technique described in Section 3.1; observe that only the elements with an edge lying on the part of the boundary

$$\Gamma_o = \{(x,0),\ x \in [0,1]\} \cup \{(0,y),\ y \in [0,1]\},$$

are modified. The link-cutting distance for the reaction-diffusion test problem (19) is given by $\sigma_{LC} = \sqrt{6\varepsilon}$ as $\min_\Gamma(b) = 1$. The final rectangular mesh is denoted by $\mathcal{P}_N^{LC}$. In Figure 2 both the initial mesh $\mathcal{P}_N$ and the final mesh $\mathcal{P}_N^{LC}$ are displayed for $\varepsilon = 10^{-4}$ and $N = 16$.

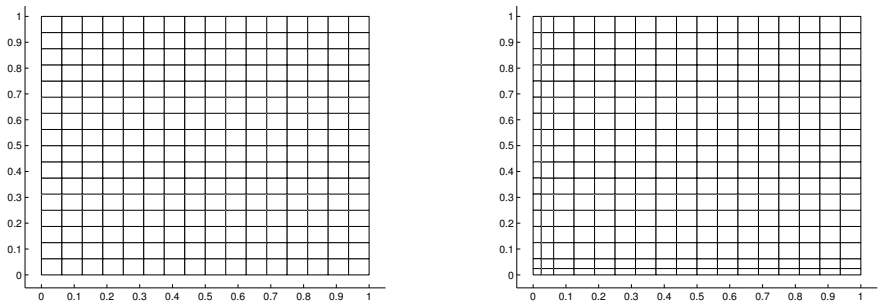

(a) Initial mesh, $\mathcal{P}_N$ (b) Modified mesh, $\mathcal{P}_N^{LC}$

Figure 2: Test problem (19) with $\varepsilon = 10^{-4}$: Initial and modified meshes via link-cutting technique for $N = 16$.

In Figure 3, we show the computed solutions with the VEM. In the left figure, the link-cutting technique is not used and then the numerical solution is obtained in the computational

mesh $\mathcal{P}_N$. We observe that this solution exhibits spurious oscillations in a similar way to the standard FEM if one does not apply the lumping technique to the mass matrix. On the other hand, if one uses the link-cutting technique a non-oscillatory solution u_N^{LC} is obtained in the computational mesh $\mathcal{P}_N^{LC}$ as it is observed in the right figure. Note that in the mesh $\mathcal{P}_N^{LC}$, the first interior mesh is located to a fixed distance (independent of the discretization parameter N) of the boundary Γ_o and then the approximation u_N^{LC} would not be improved although the mesh is refined. In the next step we deal with this drawback by solving a local problem.

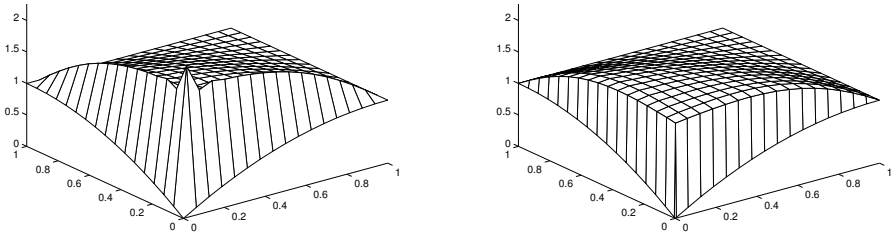

(a) Solution without link-cutting technique

(b) Solution with link-cutting technique

Figure 3: Test problem (19) with $\varepsilon = 10^{-4}$: Computed solution with VEM without and with the use of the link-cutting technique for $N = 16$.

Step 2: We shall use the following notation

$$\bar{\Omega}_{L,p} = \{(x,y) \in \Omega,\ 0 \le x \le p,\ 0 \le y \le 1\} \cup \{(x,y),\ 0 \le x \le 1,\ 0 \le y \le p\},$$

with p a positive real number to define some L-shaped subdomains of Ω.

To improve the crude approximation u_N^{LC} of the previous step in the layer region $\bar{\Omega}_{L,\sigma_{LC}}$, we use the post-processing technique described in Section 3.2. We recall that this technique is based on solving the partial differential equation (19a) posed on an L-shape subdomain $\bar{\Omega}_{L,p}$ with $p > \sigma_{LC}$. Thus, $\bar{\Omega}_{L,\sigma_{LC}} \subset \bar{\Omega}_{L,p}$. We have observed in our numerical experiences that the choice of p is not very relevant when applying this post-processing technique and we fix the value of p to be $p = 4\sigma_{LC}$ in this paper.

The values of the solution on the part of the boundary $\Gamma_{L,o} = \Gamma \cap \partial\Omega_{L,4\sigma_{LC}}$ are given in (19b) and (19c); the values of the solution on $\Gamma_{L,i} = \partial\Omega_{L,4\sigma_{LC}} \backslash \Gamma_{L,o}$ are obtained using the approximation u_N^{LC} from the first step and bilinear interpolation.

The solution of this problem is approximated with the VEM (it is not necessary now to apply the link-cutting technique) and we use a piecewise uniform mesh for both spatial variables. This mesh is defined as follows: The interval $[0,1]$ is split into two subintervals $[0, 4\sigma_{LC}]$ and $[4\sigma_{LC}, 1]$ and $N/2$ grid points are uniformly distributed within each subinterval. The final 2D mesh is the tensor product of both meshes (see Figure 4a) and it is denoted by $\bar{\Omega}^N_{L,4\sigma_{LC}}$. If we denote by z_N the computed solution in the second step, then we propose the following approximation to the solution of the test problem (19)

$$u_N = \begin{cases} u_N^{LC}, & \text{on } \mathcal{P}_N^{LC} \backslash \bar{\Omega}^N_{L,4\sigma_{LC}}, \\ z_N, & \text{on } \bar{\Omega}^N_{L,4\sigma_{LC}}. \end{cases}$$

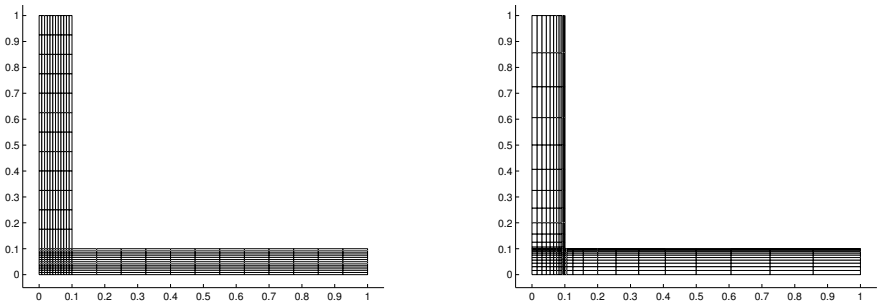

(a) Piecewise uniform mesh (b) Piecewise graded mesh

Figure 4: Mesh in the L-shaped domain $\bar{\Omega}_{L,4\sigma_{LC}}$.

We now give some information about the accuracy of the solution computed with our algorithm. The solution of the problem (19) is unknown and the orders of convergence are estimated using the two-mesh principle [10]: the finer mesh uses the grid points of the coarser mesh and their midpoints in both space variables. We denote the maximum two-mesh differences by

$$E_N = \max\left\{e_N^1, e_N^2\right\},$$

where e_N^1 and e_N^2 are the maximum two-mesh differences in the outer and inner regions

$$e_N^1 = \max_{\varphi_N^{LC}\setminus\bar{\Omega}_{L,4\sigma_{LC}}^N} \left|u_N^{LC} - u_{2N}^{LC}\right|, \quad e_N^2 = \max_{\bar{\Omega}_{L,4\sigma_{LC}}^N} |z_N - z_{2N}|.$$

Then, the orders of convergence are estimated in the usual way $Q_N = \log_2(E_N/E_{2N})$.

Note that we use the maximum norm to estimate the errors which is the appropriate norm when one considers singularly perturbed problems; we refer to [10] for a further discussion.

The numerical results are given in Table 1; observe that the maximum two-mesh differences (first row for each value of ε) are bigger for the smaller value of ε and it suggests that the method could not be uniformly convergent. In addition, for ε fixed, the orders of convergence (second row for each value of ε) are not satisfactory either since one would expect to obtain (almost) second order of convergence. To improve these numerical results, we use a

Table 1: Post-processing technique using a uniform mesh: Maximum two-mesh differences E_N and orders of convergence Q_N for the test problem (19).

	N=24	N=48	N=96	N=192
$\varepsilon = 10^{-5}$	4.901E-2	9.776E-3	2.831E-3	9.258E-4
	2.326	1.788	1.613	
$\varepsilon = 10^{-7}$	4.931E-2	1.236E-2	3.572E-3	1.418E-3
	1.996	1.791	1.333	
$\varepsilon = 10^{-9}$	4.934E-2	1.361E-2	3.773E-3	1.584E-3
	1.858	1.851	1.252	

graded mesh in the layer region $\bar{\Omega}_{L,4\sigma_{LC}}$ when the post-processing technique is applied. This type of meshes were applied in [1] to solve a singularly perturbed problem in an L-shaped domain. We also propose here to use a graded mesh, which is defined by

$$x_i = y_i = 4\sigma_{LC}\left[1 - \left(\frac{N-2i}{N}\right)^r\right], \qquad \text{for } i = 0, 1, \ldots, N/2,$$

$$x_i = y_i = 4\sigma_{LC} + (1 - 4\sigma_{LC})\left(\frac{2i-N}{N}\right)^r, \qquad \text{for } i = N/2+1, \ldots, N,$$

where $r \geq 1$ is the grading exponent. Thus, this mesh concentrates the elements at the corner $(4\sigma_{LC}, 4\sigma_{LC})$ and the final mesh for $r = 2$ is depicted in Figure 4b.

The numerical results of our scheme on the graded mesh for the choice of the grading exponent $r = 2$ are given in Table 2 and we observe an improvement compared to Table 1 where a uniform mesh was considered. Namely, the maximum two-mesh differences are stabilised as ε tends to zero and the computed orders of convergence suggest that the scheme is second order convergent. Similar numerical results have been obtained for other choices of the grading exponent with $r > 2$.

Table 2: Post-processing technique using a graded mesh: Maximum two-mesh differences E_N and orders of convergence Q_N for the test problem (19).

	N=24	N=48	N=96	N=192
$\varepsilon = 10^{-5}$	1.865E-1 2.024	4.585E-2 2.307	9.267E-3 2.122	2.129E-3
$\varepsilon = 10^{-7}$	1.882E-1 2.029	4.612E-2 2.311	9.297E-3 2.117	2.143E-3
$\varepsilon \leq 10^{-9}$	1.882E-1 2.029	4.616E-2 2.311	9.299E-3 2.117	2.144E-3

Acknowledgements

The research of J.L. Gracia was partly supported by the Institute of Mathematics and Applications (IUMA), the project MTM2013-40842-P and the Diputación General de Aragón. The research of D. Irisarri was partly supported by the Spanish MECD under FPU grant AP210-2073, the project MAT2016-76039-C4-4-R, Gobierno de Aragón and FEDER funding from the European Union (Grupo Consolidado de Mecánica de Fluidos Computacional T21)

References

[1] Andreev, V. B., and Kopteva, N. Pointwise approximation of corner singularities for a singularly perturbed reaction-diffusion equation in an *L*-shaped domain. *Math. Comp. 77*, 264 (2008), 2125–2139.

[2] Beirão da Veiga, L., Brezzi, F., Marini, L., and Russo, A. The hitchhiker's guide to the virtual element method. *Math. Mod. Meth. Appl. S. 24*, 08 (2014), 1541–1573.

[3] Beirão da Veiga, L., Brezzi, F., Marini, L., and Russo, A. Mixed virtual element methods for general second order elliptic problems on polygonal meshes. *M2AN 50*, 3 (2016), 727–747.

[4] Beirão Da Veiga, L., Brezzi, F., and Marini, L. D. Virtual elements for linear elasticity problems. *SIAM J. Numer. Anal. 51*, 2 (2013), 794–812.

[5] Beirão da Veiga, L., Brezzi, F., Cangiani, A., Manzini, G., Marini, L., and Russo, A. Basic principles of virtual element methods. *Math. Mod. Meth. Appl. S. 23*, 01 (2013), 199–214.

[6] Benedetto, M., Berrone, S., Borio, A., Pieraccini, S., and Scialo, S. Order preserving SUPG stabilization for the virtual element formulation of advection–diffusion problems. *Comput. Methods in Appl. Mech. Eng. 311* (2016), 18–40.

[7] Brezzi, F., Hauke, G., Marini, L., and Sangalli, G. Link-cutting bubbles for the stabilization of convection-diffusion-reaction problems. *Math. Mod. Meth. Appl. S. 13*, 03 (2003), 445–461.

[8] Brezzi, F., and Marini, L. D. Virtual element methods for plate bending problems. *Comput. Methods in Appl. Mech. Eng. 253* (2013), 455–462.

[9] de Falco, C., and O'Riordan, E. A patched mesh method for singularly perturbed reaction-diffusion equations. In *BAIL 2008—boundary and interior layers*, vol. 69 of *Lect. Notes Comput. Sci. Eng.* Springer, Berlin, 2009, pp. 117–127.

[10] Farrell, P., Hegarty, A., Miller, J. M., O'Riordan, E., and Shishkin, G. I. *Robust computational techniques for boundary layers*. CRC Press, 2000.

[11] Han, H., and Kellogg, R. Differentiability properties of solutions of the equation $-\epsilon^2\Delta u + ru = f(x, y)$ in a square. *SIAM J. Math. Anal. 21*, 2 (1990), 394–408.

[12] Irisarri, D. Virtual element method stabilization for convection-diffusion-reaction problems using the link-cutting condition. *Calcolo 54*, 1 (2017), 141–154.

[13] Irisarri, D., and Gracia, J. L. Virtual element method for singularly perturbed reaction-diffusion problems on non-rectangular domains. In preparation.

[14] Roos, H.-G., Stynes, M., and Tobiska, L. *Robust numerical methods for singularly perturbed differential equations*, second ed., vol. 24 of *Springer Series in Computational Mathematics*. Springer-Verlag, Berlin, 2008.

José Luis Gracia
Instituto Universitario de Aplicaciones y Matemáticas (IUMA)
Department of Applied Mathematics
University of Zaragoza
jlgracia@unizar.es

Diego Irisarri
Área de Mecánica de Fluidos
Escuela de Ingeniería y Arquitectura
University of Zaragoza
dirisarri@unizar.es